TRANSIENT STABILITY ENHANCEMENT OF DFIG BASED WECS USING HYBRID ANFBSA TECHNIQUE

D. Purushothaman[1*], Dr. V. Senthil Kumar[2], S. Sakthi[3]
[1]Research Scholar, College of Engineering Guindy, Anna University, Chennai, Tamil Nadu, India
[2]Professor, Department of Electrical and Electronics Engineering, College of Engineering Guindy, Anna University, Chennai, Tamil Nadu, India
[3]Assistant Professor, Jeppiaar Engineering College, Anna University, Chennai, Tamil Nadu, India
[*]Correspondence: dpurusothaman@gmail.com

Abstract: *Improvement of transient stability of Doubly Fed Induction Generator (DFIG)-Wind Energy Conversion System (WECS) utilizing a novel hybrid technique is exhibited in this paper. The hybrid technique is the combination of adaptive neuro fuzzy interference system (ANFIS) plus bat search algorithm (BSA) named as ANFBSA strategy. Here, the proposed ANFBSA technique is made to tune the controllers of a DFIG-WECS. The BSA technique is joined to create the dataset of possible PI gain parameters in the offline way. The ANFIS is trained by utilizing the BSA based exact solution dataset and predicts the control signals in the online way. The procedure is optimized to enhance the performance of the WECS under different operating conditions. Likewise, the proposed method considers multiple parameters which are identify with the transient stability, for example, variable wind speed, measured speed, real and reactive power, threshold rotor speed respectively. Along these lines, the transient stability and control strategies of system are improved additionally the complexity is reduced with the assistance of the proposed ANFBSA technique. Now, in the MATLAB/Simulink platform the proposed ANFBSA technique is executed and the performance is assessed utilizing existing techniques like Artificial Neural Network (ANN) and Bat Search Algorithm (BSA).*

Keywords: *Transient stability, variable speed WECS, controllers, DFIG, real and reactive power*

1. Introduction

WECS is the world's major renewable energy because of its clean and renewable nature. In the future the world's energy crises can be solved by collaborating with other RES, such as solar energy. Compared to the past because of the gradual integration of non-linear loads into grid, WECS main role is the maximum wind power capturing and improving the power quality [1]. In future, power quality of WECS is developed by integrating with grid. Frequently variable speed wind generators are used because of their improved power quality, dynamic performance during grid faults and efficient energy production. On the other hand, wind farms' working principle and structure differ from conventional power plants. Thus it becomes more complex to analyze and control the power system with wind power. Therein, transient power system stability, including wind farms, is a hot issue at the moment. Currently, according to the published article [2], the power system stability including wind farms is usually investigated by simulation. The published research shows that many factors affect the power system transient stability, including the wind farm, in particular the voltage stability, such as the integration capacity, the location of the integration point, the voltage level, the former power grid structure, the wind turbine (WT) type and the control mode of wind farm, etc.

Recently most WECS have been equipped with a variable speed DFIG that can improve the wind power systems transient stability [3]. In wind power generation an increasing application has gained individual control of power. By building up the power conversion and transmission technique the power networks qualities associated with the DFIG system change from the conventional rigid network to the distributed networks and micro grids [4-9]. To improve the transient power system stability and to provide operational reliability is the common purpose of these investigations [10, 11]. However, due to the use of DFIG, the transient stability is mostly affected by the high penetration of wind power, which is considered one of the most severe disruptions.

To improve transient stability DFIGs are for the most part furnished with crowbar system. Amid faults crowbar operation secures the rotor circuit. Among the series compensating facts devices to improve the execution of the DFIG system various limiters are employed [12-14]. For minimizing the

faults current and improving transient stability the SFCL is a standout amongst the most encouraging advances. The SFCL improves the wind power system's transient stability and furthermore announced [15-17]. During normal system operation nonetheless, presents substantial system losses utilizing SFCL [18] and lessens overall efficiency of the system [19]. What's more, to improve the DFIG wind power system's transient stability the requirement for auxiliary devices can't be overlooked. What's more, to decrease the cost per unit of power it is additionally essential to keep up the efficiency of the system [20].

Enhancement of transient stability of DFIG-WECS using hybrid technique is proposed in this paper. The hybrid technique is the combination of Adaptive Neuro Fuzzy Interference System (ANFIS) plus Bat Search Algorithm (BSA) named as ANFBSA technique. Here, the proposed ANFBSA technique is made to tune the controllers of a DFIG based WECS. The remainder of the paper is depicted as pursues: Section 2 clarifies the literature review. Section 3 clarifies the modeling of the system. Area 4 depicts the transient stability analysis of a microgrid. Section 5 depicts the proposed methodology. Section 6 portrays the simulation results and discussion. Section 7 finishes up the manuscript.

2. Recent Research Works: A Brief Review

In the related literature different review works have just existed relied upon the DFIG based WECS system utilizing different strategies and different viewpoints for the enhancement of transient stability. Some of the works are looked into on here.

Islam M.R. et al. [21] have researched the effect of expanding the switching frequency of DFIG power converters during fault conditions and this switching frequency control (SFC) procedure has been joined with Parallel Resonance Fault Current Limiter (PRFCL) to improve DFIG fault ride. Hossain M.E. et al. [22] have proposed bridge type fault current limiter (NC-NBFCL) based non-linear controller to expand the transient stability of the 20 MW wind farm (WF) based dual fed induction generator (DFIG).

Hossain M.E. et al. [23] have examined a diode-bridge-type non superconductor fault current limiter (NSFCL) to accomplish the transient stability. Hossain M.E. et al. [24] have examined the transient stability improvement analysis of DFIG based variable speed wind generator (WG). Among the FCLs series as far as practicality of execution, control structure, transient stability execution, and cost, the transient stability analysis was done. Among the series compensating devices to exhibit the transient performance of stability a temporary balanced and unbalanced failure was connected in the DFIG-based test system. Solid state fault current limiter (N-SSFCL) to improve the transient stability of DFIG based WG was exhibited by Hossain M.E. et al. [25].

2.1. Background of the Research Work

The generic analysis of the recent research work shows that a significant contributing factor in the power system is the transient stability enhancement for DFIG-based WECS. However, the voltage issue directly affects the wind farm's active power and transient stability, which further affects the power system’s active power balance and angle stability. As of late few research and development activities have been embraced to improve DFIG-based WG's transient stability. In light of DFIG to improve the transient stability of wind power systems different energy storage systems, reactive power compensators have been proposed with ongoing advances in electronic power systems. They are superconducting fault current limiter (SFCL) and flywheel energy storage (FES). A portion of these current devices have surprising expense of installation and maintenance while the above solutions can improve transient stability. To restrict the fault current and increment the power network quality experiments on NSFCL were led so as to lessen the SFCL's high technology cost. Be that as it may, NSFCL was not connected on DFIG-WECS to expand the transient stability. Along these lines requires a promising arrangement so as to improve transient stability and to defeat these difficulties utilizing DFIG- WECS system. To take care of this issue not very many methodologies based works are introduced in literature and these disadvantages and issues have inspired to do this research work.

3. System Modelling

In this section, the mathematical modelling of WECS based DFIG system and its controllers are briefly discussed. The mathematical modelling of WECS is given as follows,

3.1. WECS Modelling

The mathematical modelling of horizontal axis wind turbine has been considered for this study.

$$P_m = 0.5\, a_{den} \pi r^2 N_{wind}^2 B_c(\mu, \delta) \quad (1)$$

Here, air density can be specified as a_{den}, Radius of the turbine blades can be represented as r, speed of the wind can be specified as N_{wind}, Betz constant is $B_c(\mu, \delta)$, in theory, up to 59 percent of wind power extracted, according to Betz [30].

$$\mu = \frac{r\omega}{N_{wind}} \quad (2)$$

Here, turbine mechanical angular velocity in rad/s can be represented as ω. Non-linear functions can estimate the turbine characteristics with the aerodynamics power conversion coefficient [31].

$$B_c(\mu, \delta) = b_1\left(\frac{b_2}{\mu_i} - b_3\delta - b_4\right)e^{-b_5/\mu_i} - b_6\mu \quad (3)$$

Here, $\mu_i = \left[\frac{1}{\mu + 0.08\delta} - \frac{0.035}{\delta^3 + 1}\right]^{-1}$

3.2. Modelling of DFIG

Double fed electrical machines consists of stator and rotor windings are nourished with AC currents. Machine stator is legitimately associated with the grid, transformer, wound rotor and converters (AC to DC and DC to AC). Two modulated voltage source converters, for example, rotor side converter (RSC) and the grid side converter (GSC), three-phase pulse width modulation (PWM) and common DC connection [32-34].

3.2.1. Controllers

DFIG's stator terminals, for example, active and reactive power control are the fundamental point of the RSC [33]. Generally DFIG controls the rotor currents utilizing a rotating frame lined up with the stator flux as the rotor is sustained by an inverter [35]. Data sources are active power terminals and reactive power terminals and control the output of both the active and reactive power. To change over the amounts of the three phases into the equivalent d and q components the park transformation is considered. To create fitting reference signals a proportional integral controller is utilized for PWM signal generator block. PWM creates pulses are utilized to switch the RSC. GSC has the data sources are DC link voltage and the rotor line reactive power and create an independent reactive power infused into the grid so as to direct the dc link voltage [36].

3.2.3. DC-link Chopper/DC Crowbar

Here, a braking resistor is given to disseminate overabundance energy during a grid failure (security). DC-link chopper or the DC crowbar is the resistor associated in series with an IGBT to the DC-link bus. To deal with a particular measure of energy during a grid failure with the set of parallel resistors sized, IGBT can control the amount of energy consumed in the resistor.

3.2.4. AC Crowbar

By applying a short circuit to the rotor terminals an AC crowbar is implemented which bypasses the RSC on the RSC (rotor side). RSC protects from over current and DC link from over voltages. Using either series diode rectifier bridge with a single external resistor, or an anti-parallel thyristors connected to rotor phase external resistors the crowbar can be built. Fig 1 depicts the proposed inverter control strategies single line diagram. Proposed overall control strategies for WECS Based DFIG single line diagram is depicted in Fig 2.

4. Stability Analysis in Microgrid

For the most part microgrid is characterized as an integrated energy system involving distributed energy resources (DERs) and multiple electrical charges working as a single and autonomous grid. Here various kinds of sources are viewed as, for example, wind, PV [37] and battery. Contingent upon the sort of microgrid diverse stability issues can be identified with the most widely recognized issues. Faults in all microgrids types produce the conspicuous transient stability issues.

In a remote microgrid a fault inside the microgrid and isolation of the faulty part of the network makes transient stability issues while the typical transient stability angle is shown by a fault and consequent insulation in a utility or facility microgrid. After severe disturbance has occurred to the machine transient stability studies involve determining whether or not synchronism is maintained. Linearization is not permissible and the nonlinear swing equation needs to be resolved in most disturbances. The brief description about the transient stability analysis with swing equations has been formulated as follows,

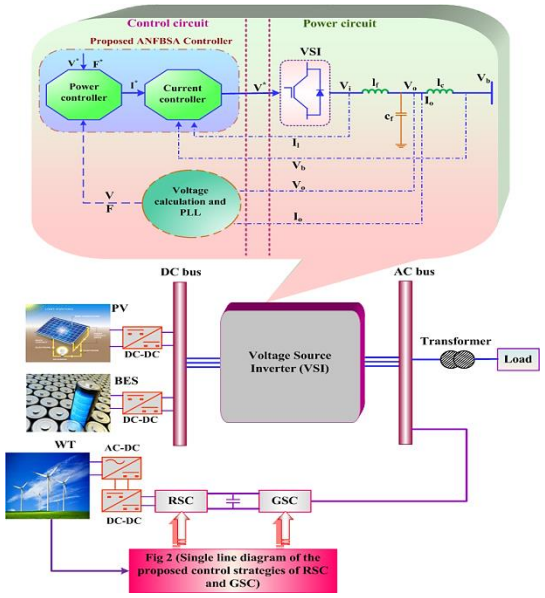

Fig. 1. Proposed inverter control strategies: Single line diagram

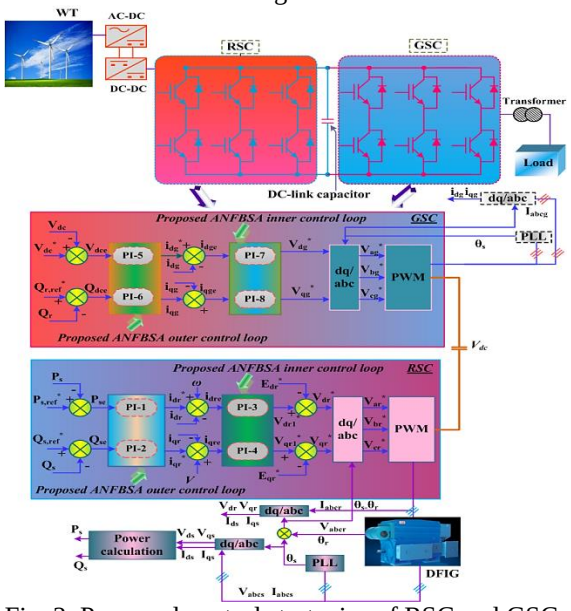

Fig. 2. Proposed control strategies of RSC and GSC: Single line diagram

4.1. Transient Stability

Synchronous power system ability to exchange stable condition and safeguard its synchronism after a sensibly large is alluded as transient stability. Consequently for power engineers to be all around familiar in the system's stability conditions and regularly, faults of such happen in the power generation systems. When all is said in done practice, in the power system transient stability considers are completed over a minimum period equivalent to the time required for one swing, which is roughly 1 sec or even less. In the event that during this first swing the system is observed to be stable and the disturbance will diminish then goes to stable.

4.1.1. Formulation of Swing Equation

The assurance of transient stability utilizing swing equation can be communicated as pursues: Here, a synchronous generator provided with mechanical torque equivalent to T_S delivered by input shaft power P_S. With an extended proportion of electromagnetic load the situation where a synchronous generator is associated out of the blue, which prompts instability by making P_E not as much as P_S as the rotor experiences deceleration. Directly to a stable condition the extended proportion of the accelerating power required is given by,

$$P_{AG} = P_S - P_E \tag{4}$$

$$T_{AG} = T_S - T_E \tag{5}$$

$$P_{AG} = T_{AG}\psi = I\alpha\psi \tag{6}$$

Here, Since T = current × angular acceleration. The equation for the angular momentum can be derived as follows,

$$AM = I\psi \tag{7}$$

$$P_{AG} = M\alpha \tag{8}$$

Loading the angular displacement fluctuates consistently with time, and it is inferred as pursues.

$$\theta = \psi_s + \frac{d\chi}{dt} \tag{9}$$

Double differentiating the above equation with respect to time, then the equation (9) becomes (10),

$$\frac{d^2\theta}{dt^2} = \frac{d^2\chi}{dt^2} \tag{10}$$

The equation for the angular acceleration is derived (11).

$$\alpha = \frac{d^2\theta}{dt^2} = \frac{d^2\chi}{dt^2} \tag{11}$$

$$P_{AG} = M\left[\frac{d^2\chi}{dt^2}\right] \tag{12}$$

$$M\frac{d^2\chi}{dt^2} = P_S - P_E \tag{13}$$

The transmitted electromagnetic power is given by,

$$\begin{aligned} P_E &= \frac{1}{X}(V_G \times V_M)\sin\chi \\ &= P_{\max}\sin\chi \end{aligned} \tag{14}$$

$$M\frac{d^2\chi}{dt^2} = P_S - P_{\max}\sin\chi \tag{15}$$

Hence the equation (15) is said to be as swing equation for the transient stability in the power system.

5. Proposed Control Methodology Based Transient Stability Analysis for Microgrid

The proposed methodology is made to tune the controllers of a DFIG-WECS. The proposed control methodology is the combination of adaptive neuro fuzzy inference system (ANFIS) and bat search algorithm (BSA). BSA is dependent on the echolocation conduct of BATS [26]. The ANFIS is one of the artificial intelligence (AI) techniques [29]. In light of an assortment of the current and power parameters the proposed technique optimally predicts the control parameters of an inner current control loop and an outer power control loop. In the offline way BSA is optimizes the pitch angle to update the transient stability of the system and delivers learning dataset. The BSA considers minimum speed variety as the objective function. The ANFIS is prepared by utilizing the BSA based exact solution dataset and predicts the control signals in the online way.

5.1. Generation of Solution Dataset Using BSA

This area depicts about the assurance of the solution dataset utilizing BSA. BSA works dependent on the echolocation behavior of bats [27, 28]. The steps for the BSA is derived as follows,

5.1.1. Steps of BSA to Generate the Dataset

Step 1: Initialization

In step 1, the input microbats are voltage, current, real and reactive power, pitch angle, frequency are initialized, which is given in the following equation (16).

$$b_i = [(X_1)^1, (X_3)^2, (X_3)^3 \cdots (X_n)^n] \tag{16}$$

Here, $(X_n)^n = P_n, Q_n, V_{dcn}, I_n, \delta_n, f_n$ are the input parameters.

Step 2: Random Generation

Randomly generate the PI controller gain parameters like K_P, K_I.

$$r^i = \begin{bmatrix} (K_pK_i)_{11} & (K_pK_i)_{12} & \cdots & (K_pK_i)_{1b} \\ (K_pK_i)_{21} & (K_pK_i)_{22} & \cdots & (K_pK_i)_{2b} \\ \vdots & \vdots & \vdots & \vdots \\ (K_pK_i)_{a1} & (K_pK_i)_{a2} & \cdots & (K_pK_i)_{ab} \end{bmatrix} \tag{17}$$

Step 3: Fitness Function

In this step, the fitness function FF_i is characterized to limit the error in view of the variation of the current and power parameters. The fitness function is depicted in the following equation.

$$FF_i = Min(\xi) \tag{18}$$

Here, error is represented as ξ.

Step 4: Randomly Updation Based on the Frequency and Velocity

Current microbats populations are updated randomly based on frequency and speed. In the following equation, the frequency and velocity calculation are explained,

$$freq_{\min} \le freq_i \le freq_{\max} \tag{19}$$

$$pulse_{\min} \le pulse_i \le pulse_{\max} \tag{20}$$

$$len_{\min} \le len_i \le len_{\max} \tag{21}$$

$$freq_i^t = freq_{\min} + (freq_{\max} - freq_{\min})u_i \tag{22}$$

$$Vel_i^t = round\left[Vel_i^{t-1} + (p_i^{t-1} - p_\gamma)u_i\right] \tag{23}$$

Here, micro-bats velocity vectors at time (*t* and *t-1*) can be specified as Vel_i^t and Vel_i^{t-1}, micro-bats position vectors at *t-1* can be specified as p_i^{t-1}, current global best solution can be represented as p_γ. The following equation portrays the neighbourhood seek in the randomly chosen population (24).

$$\rho_i^t = \rho_i^{t-1} + M_{i,j}L_{avg}^t \tag{24}$$

Here, random number between -1 and 1 can be specified as $M_{i,j}$; loudness average value at *t* can be represented as L_{avg}^t. At that point discover the objective of the new micro-bats utilizing equation

(18) and improve echolocation parameters.

Step 5: Termination

Repeat the procedure until it achieves the minimum error value or achieves the maximum number of iterations. The optimal value O of the optimization process is represented as ξ^{O} and $(K_P K_I)^{O}$. The optimal dataset of the optimization parameters are defined as follows,

$$\begin{bmatrix} (\xi)^{11} & \cdots & \cdots & (\xi)^{1n} \\ (\xi)^{21} & \cdots & \cdots & (\xi)^{2n} \\ \vdots & \vdots & \vdots & \vdots \\ (\xi)^{m1} & \cdots & \cdots & (\xi)^{mn} \end{bmatrix} = \begin{bmatrix} (K_p K_i)^{11} & (K_p K_i)^{12} & \cdots & (K_p K_i)^{1n} \\ (K_p K_i)^{21} & (K_p K_i)^{22} & \cdots & (K_p K_i)^{2n} \\ \vdots & \vdots & \vdots & \vdots \\ (K_p K_i)^{m1} & (K_p K_i)^{m2} & \cdots & (K_p K_i)^{mn} \end{bmatrix} \quad (25)$$

The optimal combination of internal and external control loop parameters like real and reactive power, voltage, current, pitch angle, frequency can therefore be demonstrated. The BSA process can be listed below,

Step 1: Initialize the generation of microbats at N dimension randomly. Here, the microbats input are the voltage, current, real and reactive power, pitch angle, frequency.

Step 2: Random generation of PI controller gain parameters.

Step 3: Fitness function evaluation is characterized to limit the error in view of the variation of the current and power parameters.

Step 4: Update the current micro-bats population randomly to update the micro-bats vector position and velocity vector. Evaluate the goal for the new population of micro-bats and select the best solution. Find the best solutions of real and reactive power, voltage, current, pitch angle, frequency.

Step 5: Check the criterion for termination if it's finished satisfied. Generate new agents for new solutions to be generated. Go to the second step.

Upon completion of the above process, the controller can be used to determine the optimum control parameters based on the parameters of the input. The ANFIS predicts optimal control signals based on the achieved dataset.

5.2. Prediction of Optimal Control Signals Using ANFIS

The ANFIS procedure is utilized to optimize the gain parameters of PI controller. Reference and actual values of real and reactive power, voltage, current, pitch angle, frequency is taken as network input and the network output is the optimal control signals. The input's non-linear function is outputs and weights that are calculated during the learning process are controlled. ANFIS is used to capture optimal PI gain parameters so that the entire machine working condition is ensured by the system. ANFIS demonstrative approach is like numerous strategies for minimizing errors. For the most part, ANFIS show has 5 layers, such as the input layer, hidden layer and output membership, the rules layer and the output layer. ANFIS is utilized to set up the BSA to copy the learning data showed to it by changing the parameters as per a chose error criterion. Fig 3 outlines the control structure of ANFIS. The steps of ANFIS arrange engineering and its hybrid learning standard is presented in this segment. By using the below condition (26) the proposed strategy objective function is assessed,

$$F = Min(e) = \begin{cases} Min\{V_{dc}^{ref} - V_{dc}\} \\ Min\{P^{ref} - P\} \\ Min\{Q^{ref} - Q\} \\ Min\{\delta^{ref} - \delta\} \\ Min\{I^{ref} - I\} \\ Min\{f^{ref} - f\} \end{cases} \quad (26)$$

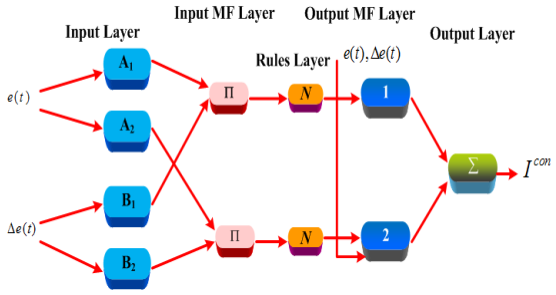

Fig. 3. Structure of ANFIS

For example, in shunt APF, e is the error evaluation between various parameters, reference dc link voltage as (V_{dc}^{ref}), real power is (P^{ref}), reactive power is (Q^{ref}), pitch angle as (δ^{ref}), current as (I^{ref}), frequency as (ϕ^{ref}) and actual dc link voltage as (V_{dc}^{act}), real power as (P), reactive power as (Q), pitch angle is (δ), current is (I),frequency as (ϕ). Two inputs and one output are present in the ANFIS structure and the inputs like error as $e(t)$ and change in error as $\Delta e(t)$ and the output is current control pulse (I^{con}). The $\Delta e(t)$ can be expressed by,

$$\Delta e = e(t) - e(t-1) \tag{27}$$

Where, error at moment state is the $e(t)$, past error condition is the $e(t-1)$, Consider first application Sugeno fuzzy inferential framework containing two standards as conditions (34) and (35),

Rule 1: If e ***is*** A_1 ***and*** Δe ***is*** B_1,

$$f_1 = a_1 x + b_1 y + c_1 \tag{28}$$

Rule 2: If e ***is*** A_2 ***and*** Δe ***is*** B_2,

$$f_2 = a_2 x + b_2 y + c_2 \tag{29}$$

Here, a_1, a_2, b_1, b_2, c_1 and c_2 are linear parameters and $A1, A2, B1$ and $B2$ are nonlinear parameter. The drawbacks of learning ability of neural networks and deduction component such as human brain given by FFA are therefore used by ANFIS. Here, delineates graphically the fluffy thinking component to get a yield from a given input vector $[e, \Delta e]$. All the more unequivocally, the yield can communicate as conditions (30),

$$I^{con} = \frac{W_1 f_1 + W_2 f_2}{W_1 + W_2} \tag{30}$$

(I^{con}) is the each normal weighted administers output. Putting the FFA into the structure of versatile networks is helpful in order to encourage the Sugeno-model learning (or adjustment), which can deliberately calculate gradient vectors. Terminals within an ANFIS layer perform comparable undertakings as shown below, which are determined by their node capacity.

Layer 1: Input layer

Layer 1: The equation for the layer 1 is depicted as follows

$$O_i^1 = \kappa_{Ai}(e); i = 1,2 \tag{31}$$

$$O_i^1 = \kappa_{Bi-2}(\Delta e); i = 3,4 \tag{32}$$

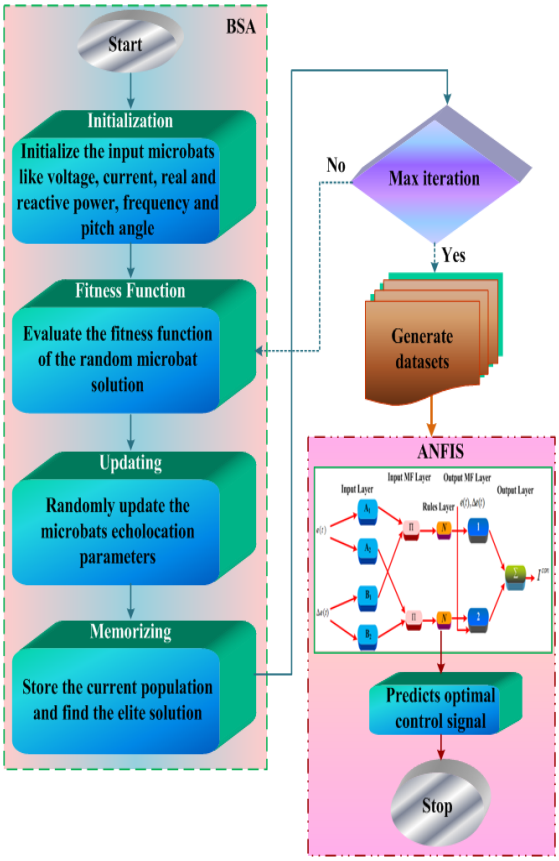

Fig. 4. Flowchart of the proposed ANFBSA technique

Where, i is the data set membership grade (A_1, B_1, A_2, B_2) and O_i^1 is the i^{th} output node in layer 1.

Layer 2: Membership Layer

Layer 2 equation is derived as follows,

$$O_i^2 = W_i = \kappa_{Ai}(e) \times \kappa_{Bi}(\Delta e), i = 1,2,...,5 \tag{33}$$

Layer 3: Rule Layer

Layer 3 equations are as follows,

$$O_i^3 = W_i = \frac{W_i}{W_1 + W_2}, i = 1,2 \tag{34}$$

Layer 4: Defuzzification Layer

Layer 4 equation is described as follows,

$$O_i^4 = W_i f_i = W_i (a_i x + b_i y + c_i), i = 1,2 \tag{35}$$

Where, W_i is a firing strength (normalized).

Layer 5: Output Layer

Layer 5 equation can be specified as follows,

$$O_i^5 = \sum_{i=1}^{2} W_i f_i = \frac{W_1 f_1 + W_2 f_2}{W_1 + W_2} \quad (36)$$

The PI controller's gain parameters are optimally tuned and the controller with the proposed technique offers reliable system operation. The flowchart of the ANFBSA technique is appeared in Fig 4.

6. Simulation Results and Discussion

In this section, the simulation results and discussion of proposed are studied and simulated using two types. The proposed technique is implemented in MATLAB/Simulation working stage. The proposed system is tested based on the deviation in the load with two types such as Type 1: load increase, Type 2: load increase and decrease and their results are compared with ANN and BSA. The proposed approach for two types is discussed as below.

6.1. Type 1

The first type of transient operation examined is the load increase transient event is the results of which are appeared and clarified using the accompanying figures.

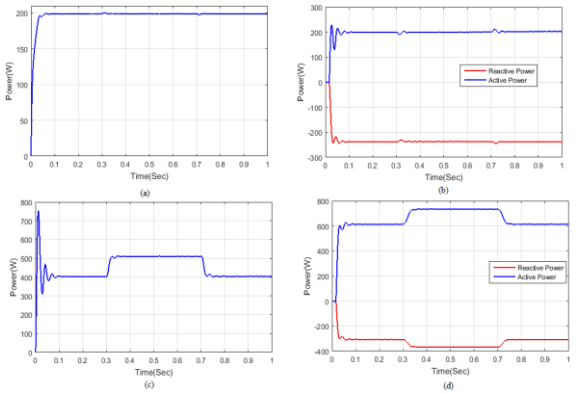

Fig. 5. Performance analysis of (a) PV (b) Wind (c) Battery (d) Load

Fig 5 shows the performance of PV, wind, battery and load under type 1. Fig 5 (a) shows the PV power with time. From the Fig 5 (a), PV power interrupts at the time instant of 0.3 and goes to the normal condition by using the proposed technique. Fig 5 (b) shows the graph of wind power versus time. From the graph the active power of wind disturbed at the time of 0.3 and instantly the system goes to the normal condition. The reactive power of wind also disturbed at the time of 0.3 and instantly the system goes to normal state. Fig 5 (c) illustrates the graph of battery power with respect to time. On the basis of Fig 5 (c), the battery power flickers at the time moment of 0.31 and after the flickering moment the system goes to the normal state. Fig 5 (d) shows the load power verses time. In view of the fig 5 (d), the load active power flickered at the moment of 0.32 and after the flicker the system works at steady condition. The load reactive power flickers at the time moment of 0.33 and instantly the system works at a reliable operating condition by using the proposed technique. Fig 6 shows the performance of PV, wind, battery and load of proposed and existing techniques. Fig 6 (a) shows the performance comparison of PV of proposed and existing techniques. By observing fig 6(a), the PV power of base method flickered at the time range from 0.3 to 0.315sec. The PV power of ANN technique interrupts at the time moment of 0.3 to 0.31sec. The PV power of BSA technique flickers at t=0.3 to 0.31 sec. The power in the PV flickers at the time instant of 0.3 sec, instantly the flicker is resolved and the system goes to the normal working condition. Fig 6 (b) shows the wind power with time. From the figure, the wind power of base method scattered at the time moment of 0.3 to 0.34 sec. The wind power of ANN technique flicker at the range of 0.3 to 0.33 sec. The wind power of BSA technique interrupted at the time range of 0.3 to 0.32 sec. The wind power of proposed technique flickered and instantly the problem is resolved and goes to normal state. Fig 6 (c) delineates the battery power of base technique versus time. At the time of 0.3 to 0.33 sec the base technique gives the maximum battery power of 550 and after that time instant the power gets drop and system goes to abnormal condition. The battery power using ANN technique achieves the maximum power at the time instant of 0.31 to 0.33 sec. The battery power of BSA technique acquires the maximum power of 530 W at the time range of 0.32 to 0.33 sec. The proposed technique achieves the maximum power of 510 W at the time moment of 0.3sec. At the time of 0.3sec the flicker happens and there is no power deviation in the system because the proposed system eliminates the flickers instantly and operates the system with normal condition. Fig 6 (d) depicts the load power of proposed and existing techniques versus time. As seen from the fig 6 (d), the base method of load power scattered at the time moment of 0.33 to 0.35 sec. The ANN technique of load power flickers at the time range of 0.34 to 0.35 sec. The load power using BSA technique disturbed at the time range of 0.34 to 0.35 sec. The load power of proposed technique achieves better result with less distortion in the load power than the existing techniques.

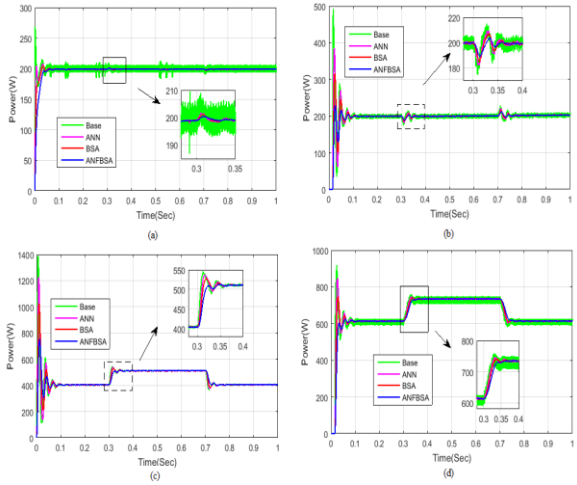

Fig. 6. Comparison analysis of (a) PV (b) Wind (c) Battery (d) Load

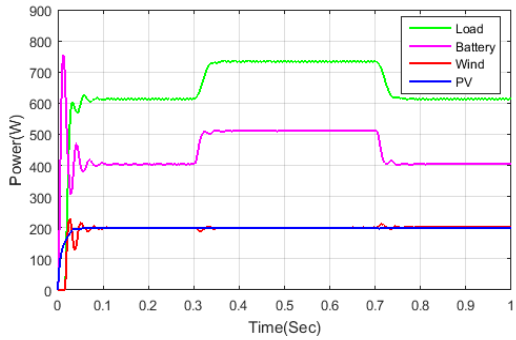

Fig. 7. Total resources power comparison

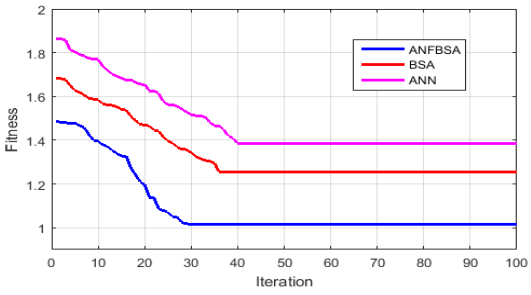

Fig. 8. Fitness comparison

Fig 7 shows the total power comparison of proposed technique versus time. By observing the fig 7, the PV power distorted at the time moment of 0.3 sec. The wind power flickers at the instant of time and finally goes to the normal condition instantly. The battery power scattered at the time instant of 0.32 sec and after the interruption the system working under the normal state. The load power scattered at the minute deviation and after the minute deviation instantly the proposed technique clear up the interruption and activates the system to work in a normal condition. Fig 8 shows the fitness graph of proposed and existing techniques. From the fig 8, ANN converges at the iteration range of 40; BSA converged at the iteration range of 35. But the proposed technique converges quickly at the iteration count of 28 and the graph finally shows that the proposed technique has easily converges than the existing techniques. Table 1 shows the statistical analysis for type 1. It is observed from the Table 1 it is observed that the proposed technique has the optimal solution than the existing techniques.

Table. 1. Statistical Analysis for Type 1

Solution Techniques	Mean	Median	SD
ANFBSA	1.0935	1.0159	0.1504
BSA	1.3372	1.2558	0.1323
ANN	1.4844	1.3862	0.1482
Base	1.6084	1.4829	0.1911

6.2. Type 2

The second type of transient operation investigated is the load increase and decrease transient event is the results of which are shown as follows: Performance of PV, wind, battery and load under type 2 is depicted in Fig 9. Fig 9 (a) shows the PV power versus time. From the Fig 9 (a), PV power increased at the time instant of 0.3 and goes to the normal condition by using the proposed technique. and at the time moment of 0.6 the PV power decreased and goes to the operating condition. Fig 9 (b) shows the graph of wind power versus time. Wind active power decreased at t= 0.2 instantly the system goes to the operating condition and at the time instant of 0.4 the active power of wind increased and instantly turns to the normal condition. The reactive power of wind also decreased at the time of 0.2 and the system goes to normal state. At the time instant of 0.4 the active power of wind increased and instantly turns to the normal condition. Fig 9 (c) illustrates the graph of battery power with respect to time. On the basis of Fig 9 (c), the battery power decreased at the time moment of 0.21 and after the flickering moment the system goes to the normal state. At the time instant of 0.4 the battery power increased and instantly turns to the normal condition. Fig 9 (d) shows the load power verses time. In view of the fig 9 (d), the load active power decreased at the moment of 0.22 and after the flicker the system works at steady condition. The load active power increased at the time range of 0.42 sec then the system works at steady condition. The load reactive power increased at the time moment of 0.22 and instantly the system works at a reliable operating condition by using the proposed technique. The load

reactive power decreased at the moment of 0.42 and after the flicker the system works at steady condition.

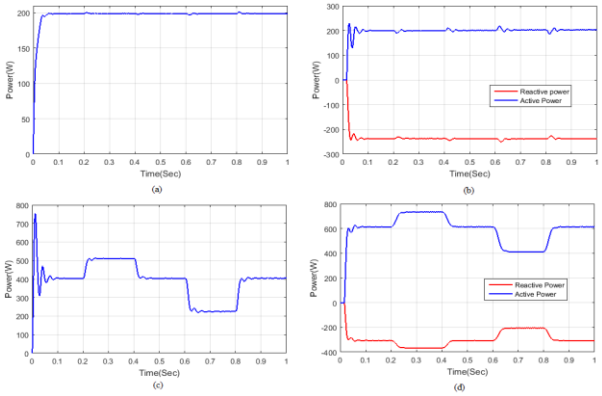

Fig. 9. Performance analysis of (a) PV (b) Wind (c) Battery (d) Load

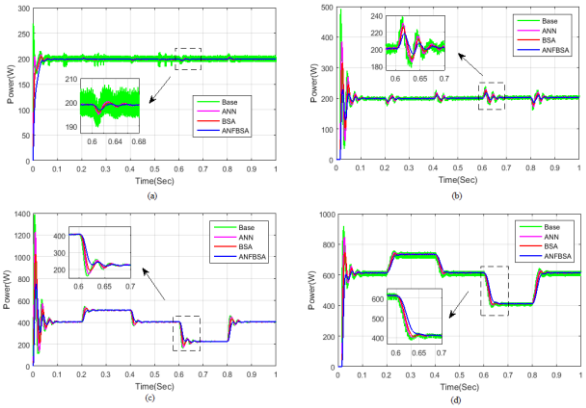

Fig 10: Comparison analysis of (a) PV (b) Wind (c) Battery (d) Load

Fig 10 shows the performance of PV, wind, battery and load of proposed and existing techniques. Fig 10 (a) depicts the performance comparison of PV of proposed and existing techniques. By observing the fig 10 (a), the PV power of base method decreased at the time range from 0.6 to 0.64 sec and increased at the time of 0.64 to 0.66 sec. The PV power of ANN technique increased at the time moment of 0.6 to 0.64sec. The PV power decreased at the time range of 0.65 to 0.67 sec. The PV power of BSA technique increased at t=0.6 to 0.63 sec. The BSA PV power decreased at the time moment of 0.64 to 0.65 sec. The PV power of the proposed technique flickers at the time instant of 0.6 sec, instantly the flicker is resolved and the system goes to the normal working condition. Fig 10 (b) shows the wind power with time. From the figure, the wind power of base method increased at the time moment of 0.6 to 0.63 sec. The wind power of base method decreased at the time moment of 0.63 to 0.65 sec. The wind power of ANN technique increased at the range of 0.6 to 0.64 sec. The wind power of ANN technique decreased at the range of 0.64 to 0.66 sec. The wind power of BSA technique increased at the time range of 0.6 to 0.63 sec. The wind power of BSA technique decreased at the time range of 0.63 to 0.64 sec. The wind power of proposed technique flickered and instantly the problem is resolved and goes to normal state. Fig 10 (c) delineates the battery power versus time. At the time of 0.6 to 0.63 sec the base technique gives the maximum battery power of 400 and after that time instant the power gets drop and system goes to abnormal condition. The battery power using ANN technique achieves the maximum power at the time instant of 0.6 to 0.635 sec. The battery power of BSA technique acquires the maximum power of 400 W at the time range of 0.6 to 0.62 sec. The proposed technique achieves the maximum power at the time moment of 0.6 sec. At the time of 0.6 sec the flicker happens and there is no power deviation in the system. Fig 10 (d) depicts the load power of proposed and existing techniques versus time. The load power of proposed technique achieves better result with less distortion while increasing and decreasing of load power than the existing techniques.

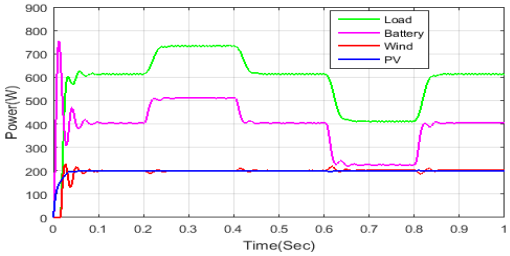

Fig. 11. Total resources power comparison

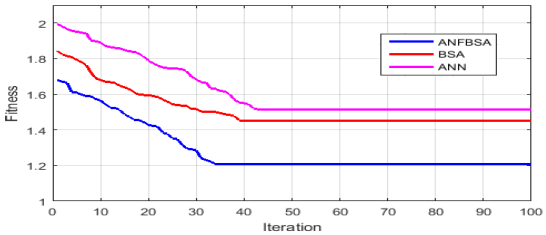

Fig. 12. Fitness comparison

Fig 11 shows the total power comparison of proposed technique versus time. By observing the fig 11, the PV power flickers at the instant of time and finally goes to the normal condition instantly. The wind power decreased at the time moment of 0.2 sec and the PV power increased at the time moment of 0.41 sec. Then battery power increased at the time instant of 0.42 sec and after the interruption the system working under the normal state.

The load power scattered at the minute deviation and after it clear up the interruption and activates the

system to work in a normal condition. Fig 12 shows the fitness graph of proposed and existing techniques. Table 2 shows the statistical analysis for type 2. It confirms that the proposed technique has the optimal solution over the other techniques. Fig 13 shows computational time of proposed with existing techniques for Type 1 and Type 2.

Table. 2. Statistical Analysis for Type 2

Methods	Mean	Median	SD
ANFBSA	1.2909	1.2077	0.1416
BSA	1.5138	1.4500	0.1061
ANN	1.6222	1.5146	0.1546
Base	1.7767	1.6201	0.2173

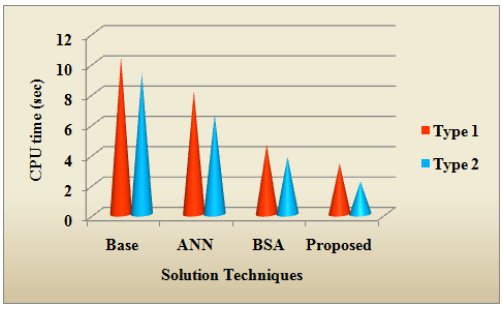

Fig. 13. Computational time of proposed and existing techniques

As seen from the Fig 13, the proposed technique achieves optimal solution with less computation time when comparing with the existing techniques. Therefore, the control strategies of the system and the transient stability are improved and also the complexity is reduced with the help of the proposed ANFBSA technique.

7. Conclusion

A hybrid technique is introduced to enhance the transient stability of DFIG-WECS. For re-establishing the normal operating condition of the power system, the proposed ANFBSA technique is used. The proposed strategy optimally predicts the PI gain parameters in light of a variety of the current and power parameters. The proposed controller is completed in the MATLAB/Simulink platform. By using the proposed methodology, the transient stability is enhanced simultaneously to improve the DFIG based WECS. Moreover, the proposed controller yields a competitive performance regarding CPU time, statistical analysis. The results confirm that the system produces stable and reliable operation utilizing the proposed methodology. In this manner, the proposed strategy is a promising procedure for deciding complicated issues with accurate results and the controller offers reliable operation of the system.

References

[1] Wang, L., Truong, D.: *Stability Enhancement of a Power System With a PMSG-Based and a DFIG-Based Offshore Wind Farm Using a SVC With an Adaptive-Network-Based Fuzzy Inference System*. IEEE Transactions on Industrial Electronics, vol. 60, no. 7, 2013, pp. 2799-2807.

[2] Wang, L., Truong, D.: *Stability Enhancement of DFIG-Based Offshore Wind Farm Fed to a Multi-Machine System Using a STATCOM*. IEEE Transactions on Power Systems, vol. 28, no. 3, 2013, pp. 2882-2889.

[3] Kailasa Gounder, Y., Boominathan, V., Nanjundappan, D.: *Enhancement of transient stability of distribution system with SCIG and DFIG based wind farms using STATCOM*. IET Renewable Power Generation, vol. 10, no. 8, 2016, pp. 1171-1180.

[4] Mehta, B., Bhatt, P., Pandya, V.: *Small signal stability enhancement of DFIG based wind power system using optimized controllers parameters*. International Journal of Electrical Power & Energy Systems, vol. 70, 2015, pp. 70-82.

[5] Hossain, M., Ali, M.: *Transient stability improvement of doubly fed induction generator based variable speed wind generator using DC resistive fault current limiter*. IET Renewable Power Generation, vol. 10, no. 2, 2016, pp. 150-157.

[6] Tang, Y., He, H., Wen, J., Liu, J.: *Power System Stability Control for a Wind Farm Based on Adaptive Dynamic Programming*. IEEE Transactions on Smart Grid, vol. 6, no. 1, 2015, pp. 166-177.

[7] Meegahapola, L., Littler, T., Perera, S.: *Capability curve based enhanced reactive power control strategy for stability enhancement and network voltage management*. International Journal of Electrical Power & Energy Systems, vol. 52, 2013, pp. 96-106.

[8] Hussein, A., Hasan Ali, M.: *Comparison among series compensators for transient stability enhancement of doubly fed induction generator based variable speed wind turbines*. IET Renewable Power Generation, vol. 10, no. 1, 2016, pp. 116-126.

[9] Taj, T., Alolah, A., Hasanien, H., Muyeen, S.: *Transient stability enhancement of a grid-connected wind farm using an adaptive neuro-fuzzy controlled-flywheel energy storage system*. IET Renewable Power Generation, vol. 9, no. 7, 2015, pp. 792-800.

[10] Hossain, M.: *A non-linear controller based new bridge type fault current limiter for transient stability enhancement of DFIG based Wind Farm*. Electric Power Systems Research, vol. 152, 2017, pp. 466-484.

[11] Muyeen, S., Hasanien, H., Al-Durra, A.: *Transient stability enhancement of wind farms connected to a*

multi-machine power system by using an adaptive ANN-controlled SMES. Energy Conversion and Management, vol. 78, 2014, pp. 412-420.

[12] Hossain, M.: *RETRACTED: A new approach for transient stability improvement of a grid-connected doubly fed induction generator–based wind generator.* Wind Engineering, vol. 41, no. 4, 2017, pp. 245-259.

[13] Patnaik, R., Dash, P., Mahapatra, K.: *Adaptive terminal sliding mode power control of DFIG based wind energy conversion system for stability enhancement.* International Transactions on Electrical Energy Systems, vol. 26, no. 4, 2015, pp. 750-782.

[14] Rashid, G., Ali, M.: *Transient Stability Enhancement of Doubly Fed Induction Machine-Based Wind Generator by Bridge-Type Fault Current Limiter*. IEEE Transactions on Energy Conversion, vol. 30, no. 3, 2015, pp. 939-947.

[15] Kanchanaharuthai, A., Chankong, V., Loparo, K.: *Transient Stability and Voltage Regulation in Multimachine Power Systems Vis-à-Vis STATCOM and Battery Energy Storage*. IEEE Transactions on Power Systems, vol. 30, no. 5, 2015, pp. 2404-2416.

[16] Hossain, M., Ali, M.: *Transient Stability Augmentation of PV/DFIG/SG-Based Hybrid Power System by Nonlinear Control-Based Variable Resistive FCL*. IEEE Transactions on Sustainable Energy, vol. 6, no. 4, 2015, pp. 1638-1649.

[17] Routray, S., Patnaik, R., Dash, P.: *Adaptive Non-Linear Control of UPFC for Stability Enhancement in a Multimachine Power System Operating with a DFIG Based Wind Farm*. Asian Journal of Control, vol. 19, no. 4, 2017, pp. 1575-1594.

[18] Kenan Döşoğlu, M.: *Hybrid low voltage ride through enhancement for transient stability capability in wind farms*. International Journal of Electrical Power & Energy Systems, 2019, pp.655-662.

[19] Firouzi, M., Gharehpetian, G., Salami, Y.: *Active and reactive power control of wind farm for enhancement transient stability of multi-machine power system using UIPC*. IET Renewable Power Generation, vol. 11, no. 8, 2017, pp. 1246-1252.

[20] Shi, L., Sun, S., Yao, L., Ni, N., Bazargan, M.: *Effects of wind generation intermittency and volatility on power system transient stability*. IET Renewable Power Generation, vol. 8, no. 5, 2014, pp. 509-521.

[21] Islam, R., R. I, M., Sheikh, M.: *Transient Stability Enhancement of DFIG based Wind Generator by Switching Frequency Control Strategy with Parallel Resonance Fault Current Limiter*. Global Journal of Research In Engineering, vol 18, no 1-F, 2018.

[22] Hossain, M.: *A non-linear controller based new bridge type fault current limiter for transient stability enhancement of DFIG based Wind Farm*. Electric Power Systems Research, vol. 152, 2017, pp. 466-484.

[23] Hossain, M.: *Performance analysis of diode-bridge-type non-superconducting fault current limiter in improving transient stability of DFIG based variable speed wind generator*. Electric Power Systems Research, vol. 143, 2017, pp. 782-793.

[24] Hossain, M.: *Transient stability improvement analysis among the series fault current limiters for DFIG based wind generator.* 2017 19th International Conference on Intelligent System Application to Power Systems (ISAP), 17-20, Sep 2017, San Antonio, TX, USA, pp. 1-6.

[25] Hossain, M.: *Performance of new solid-state fault current limiter for transient stability enhancement of DFIG based wind generator*. 2017 North American Power Symposium (NAPS), 17-19, Sep 2017, Morgantown, WV, USA, pp. 1-6.

[26] Ali, E.: *Optimization of Power System Stabilizers using BAT search algorithm.* International Journal of Electrical Power & Energy Systems, vol. 61, 2014, pp. 683-690.

[27] Kumar, B., Srikanth, N.: *Bat Algorithm and Firefly Algorithm f or Improving Dynamic Stability of Power Systems Using UPFC*. International Journal on Electrical Engineering and Informatics, vol. 8, no. 1, 2016, pp. 164-188.

[28] Sakthivel, S., Natarajan, R., Gurusamy, P.: *Application of Bat Optimization Algorithm for Economic Load Dispatch Considering Valve Point Effects.* International Journal of Computer Applications, vol. 67, no. 11, 2013, pp. 35-39.

[29] Mishra, R., Mohanty, K.: *Real time implementation of an ANFIS-based induction motor drive via feedback linearization for performance enhancement.* Engineering Science and Technology, an International Journal, vol. 19, no. 4, 2016, pp. 1714-1730.

[30] Varol, A., İlkılıç, C., Varol, Y.: *Increasing the efficiency of wind turbines*. Journal of Wind Engineering and Industrial Aerodynamics, vol. 89, no. 9, 2001, pp. 809-815.

[31] El-Shimy, M.: *Modeling and analysis of reactive power in grid-connected onshore and offshore DFIG-based wind farms*. Wind Energy, vol. 17, no. 2, 2012, pp. 279-295.

[32] Tapia, A., Tapia, G., Ostolaza, J., Saenz, J.: *Modeling and control of a wind turbine driven doubly fed induction generator*. IEEE Transactions on Energy Conversion, vol. 18, no. 2, 2003, pp. 194-204.

[33] Mohammadi, J., Vaez-Zadeh, S., Afsharnia, S., Daryabeigi, E.: *A Combined Vector and Direct Power Control for DFIG-Based Wind Turbines*. IEEE Transactions on Sustainable Energy, vol. 5, no. 3, 2014, pp. 767-775.